Accepted Manuscript

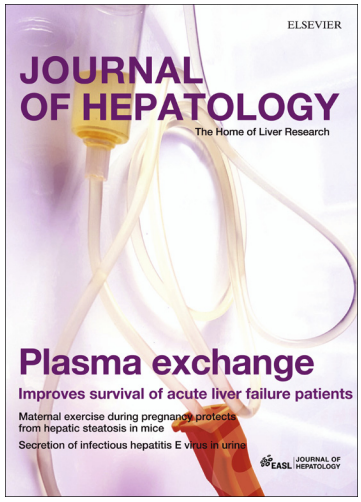

Ammonia produces pathological changes in human hepatic stellate cells and is a target of therapy of portal hypertension

Rajiv Jalan, Francesco De Chiara, Vairappan Balasubramaniyan, Fausto Andreola, Varun Khetan, Massimo Malago, Massimo Pinzani, Rajeshwar P. Mookerjee, Krista Rombouts

PII: S0168-8278(15)00777-1
DOI: http://dx.doi.org/10.1016/j.jhep.2015.11.019
Reference: JHEPAT 5902

To appear in: *Journal of Hepatology*

Received Date: 8 June 2015
Revised Date: 9 November 2015
Accepted Date: 11 November 2015

Please cite this article as: Jalan, R., De Chiara, F., Balasubramaniyan, V., Andreola, F., Khetan, V., Malago, M., Pinzani, M., Mookerjee, R.P., Rombouts, K., Ammonia produces pathological changes in human hepatic stellate cells and is a target of therapy of portal hypertension, *Journal of Hepatology* (2015), doi: http://dx.doi.org/10.1016/j.jhep.2015.11.019

AMMONIA PRODUCES PATHOLOGICAL CHANGES IN HUMAN HEPATIC STELLATE CELLS AND IS A TARGET OF THERAPY OF PORTAL HYPERTENSION

Running title : ammonia and hepatic stellate cells

Rajiv Jalan[*], Francesco De Chiara[*], Vairappan Balasubramaniyan, Fausto Andreola, Varun Khetan, Massimo Malago[#], Massimo Pinzani, Rajeshwar P. Mookerjee[&] and Krista Rombouts[&].

[*]Jalan and De Chiara are joint 1st authors

[&]Rombouts and Mookerjee are joint Senior authors

Liver Failure Group, Institute for Liver & Digestive Health, University College of London, Royal Free, London, UK. [#]Division of Surgery, University College London, Royal Free London, UK.

Corresponding authors:

Krista Rombouts PhD. Royal Free Hospital & University College London UCL, Institute for Liver & Digestive Health, Division of Medicine, Rowland Hill Street, London, NW3 2PF, United Kingdom

Phone: +44 02074332794; Fax: +44 02074332852

E-mail: k.rombouts@ucl.ac.uk

Rajeshwar P. Mookerjee MD PhD. Royal Free Hospital & University College London UCL, Institute for Liver & Digestive Health, Division of Medicine, Rowland Hill Street, London, NW3 2PF, United Kingdom.

Phone: +44 02074332792; Fax: +44 02074332852

Email: r.mookerjee@ucl.ac.uk

Word count: 6484

Number of figures and tables: 7 figures

List of abbreviations:

3-NTyrosine	3-Nitrotyrosine
α-SMA	alpha Smooth Muscle Actin
AAs	Amino acid-rich
ATF6	Activating transcription factor 6
BDL	Bile Duct Ligation
BIP	Immunoglobulin heavy chain binding protein
BrdU	5-Bromo-2-Deoxyuridine
carboxy-DCF	(5(6)-Carboxy-2',7'-dichlorofluorescein
carboxy-H2DCFDA	2',7'-dichlorodihydrofluorescein diacetate
CCL2	Chemokine (C-C motif) ligand 2
CHOP	CCAAT-enhancer-binding protein homologous protein
CM	Complete Medium
Col1A1	Collagen type I alpha 1
DAPI	4',6-diamidino-2-phenylindole
ELISA	Enzyme-Linked Immunosorbent Assay

eNOS	Endothelial Nitric Oxide Synthase
ER	Endoplasmic Reticulum
ET1	Endothelin 1
GFAP	Glial Fibrillary Acidic Protein
GS	Glutamine Synthetase
HE	Hepatic Encephalopathy
hHSC	Human Hepatic Stellate Cells
HPRT1	Hypoxanthine phosphoribosyltransferase 1
IL1β	Interleukin-1 beta
IL6	Interleukin-6
IL8	Interleukin-8
iNOS	Inducible Nitric Oxide Synthase
LOX	Lysyl oxidase
MAP	Mean arterial pressure
MMP2	Matrix metalloproteinase-2
mRNA	Messenger RNA
MSO	L-Methionine sulfoximine
MTS	(4-sulfophenyl)-2H-tetrazolium, inner salt)
NFkB	Nuclear Factor kappa B
NH4Cl	Ammonium Chloride
OP	Ornithine Phenylacetate
p38MAPK	p38 mitogen-activated protein kinases
PDGF-Rβ	Platelet derived growth factor receptor-β
RNA	Ribonucleic Acid
ROS	Reactive Oxygen Species

SEM	Standard Error of the Mean
SFM	Serum Free Medium
SOD2	Superoxide dismutase 2
TGFbeta1	Transforming Growth Factor Beta 1
TIMP-1	Metallopeptidase inhibitor 1
TRITC	Tetramethylrhodamine
XBP1	X-box binding protein 1

Keywords: human hepatic stellate cells, (hHSC); Ammonia; glutamine synthetase, (GS); Ornithine Phenylacetate, (OP); Bile Duct Ligation, (BDL); Endoplasmic reticulum stress, (ER); oxidative stress; Hepatic Encephalopathy (HE)

Conflict of interest: Rajiv Jalan has served on Scientific Advisory Board for Conatus Pharma, has received lecture fees from Gambro and has on-going research collaboration with Gambro, Grifols and is the Principal Investigator of an Industry sponsored study (Sequana Medical). He is also inventor for a drug, L-ornithine phenyl acetate (OP) (OCR-002) which UCL has licensed to Ocera Therapeutics. He is also the founder of UCL spin-out company Yaqrit ltd. and Cyberliver ltd.

All other authors have nothing to disclose.

Author contributions:

(1) conception and design of the study; RJ, RPM, KR designed the study.

(2) generation, collection, assembly, analysis and/or interpretation of data; FDC, FA, VB, VK and KR.

(3) drafting of the manuscript; RJ, FDC, FA, RPM, KR

(4) critical revision of the manuscript; MP, MM

(5) approval of the final version of the manuscript; All authors and all authors approved the authorship list.

AMMONIA PRODUCES PATHOLOGICAL CHANGES IN HUMAN HEPATIC STELLATE CELLS AND IS A TARGET OF THERAPY OF PORTAL HYPERTENSION

Running title : ammonia and hepatic stellate cells

Rajiv Jalan[*], Francesco De Chiara[*], Vairappan Balasubramaniyan, Fausto Andreola, Varun Khetan, Massimo Malago[#], Massimo Pinzani, Rajeshwar P. Mookerjee[&] and Krista Rombouts[&].

[*]Jalan and De Chiara are joint 1st authors

[&]Rombouts and Mookerjee are joint Senior authors

Liver Failure Group, Institute for Liver & Digestive Health, University College of London, Royal Free, London, UK. [#]Division of Surgery, University College London, Royal Free London, UK.

Corresponding authors:

Krista Rombouts PhD. Royal Free Hospital & University College London UCL, Institute for Liver & Digestive Health, Division of Medicine, Rowland Hill Street, London, NW3 2PF, United Kingdom

Phone: +44 02074332794; Fax: +44 02074332852

E-mail: k.rombouts@ucl.ac.uk

Rajeshwar P. Mookerjee MD PhD. Royal Free Hospital & University College London UCL, Institute for Liver & Digestive Health, Division of Medicine, Rowland Hill Street, London, NW3 2PF, United Kingdom.

Phone: +44 02074332792; Fax: +44 02074332852

Email: r.mookerjee@ucl.ac.uk

Keywords: human hepatic stellate cells, (hHSC); Ammonia; glutamine synthetase, (GS); Ornithine Phenylacetate, (OP); Bile Duct Ligation, (BDL); Endoplasmic reticulum stress, (ER); oxidative stress; Hepatic Encephalopathy (HE)

Word count: 6484

Number of figures and tables: 7 figures

List of abbreviations:

3-NTyrosine	3-Nitrotyrosine
α-SMA	alpha Smooth Muscle Actin
AAs	Amino acid-rich
ATF6	Activating transcription factor 6
BDL	Bile Duct Ligation
BIP	Immunoglobulin heavy chain binding protein
BrdU	5-Bromo-2-Deoxyuridine
carboxy-DCF	(5(6)-Carboxy-2',7'-dichlorofluorescein
carboxy-H2DCFDA	2',7'-dichlorodihydrofluorescein diacetate
CCL2	Chemokine (C-C motif) ligand 2
CHOP	CCAAT-enhancer-binding protein homologous protein
CM	Complete Medium

Col1A1	Collagen type I alpha 1
DAPI	4',6-diamidino-2-phenylindole
ELISA	Enzyme-Linked Immunosorbent Assay
eNOS	Endothelial Nitric Oxide Synthase
ER	Endoplasmic Reticulum
ET1	Endothelin 1
GFAP	Glial Fibrillary Acidic Protein
GS	Glutamine Synthetase
HE	Hepatic Encephalopathy
hHSC	Human Hepatic Stellate Cells
HPRT1	Hypoxanthine phosphoribosyltransferase 1
IL1β	Interleukin-1 beta
IL6	Interleukin-6
IL8	Interleukin-8
iNOS	Inducible Nitric Oxide Synthase
LOX	Lysyl oxidase
MAP	Mean arterial pressure
MMP2	Matrix metalloproteinase-2
mRNA	Messenger RNA
MSO	L-Methionine sulfoximine
MTS	(4-sulfophenyl)-2H-tetrazolium, inner salt)
NFkB	Nuclear Factor kappa B
NH4Cl	Ammonium Chloride
OP	Ornithine Phenylacetate
p38MAPK	p38 mitogen-activated protein kinases

PDGF-Rβ	Platelet derived growth factor receptor-β
RNA	Ribonucleic Acid
ROS	Reactive Oxygen Species
SEM	Standard Error of the Mean
SFM	Serum Free Medium
SOD2	Superoxide dismutase 2
TGFbeta1	Transforming Growth Factor Beta 1
TIMP-1	Metallopeptidase inhibitor 1
TRITC	Tetramethylrhodamine
XBP1	X-box binding protein 1

Conflict of interest: Rajiv Jalan has served on Scientific Advisory Board for Conatus Pharma, has received lecture fees from Gambro and has on-going research collaboration with Gambro, Grifols and is the Principal Investigator of an Industry sponsored study (Sequana Medical). He is also inventor for a drug, L-ornithine phenyl acetate (OP) (OCR-002) which UCL has licensed to Ocera Therapeutics. He is also the founder of UCL spin-out company Yaqrit ltd. and Cyberliver ltd.

All other authors have nothing to disclose.

Author contributions:

(1) conception and design of the study; RJ, RPM, KR designed the study.

(2) generation, collection, assembly, analysis and/or interpretation of data; FDC, FA, VB, VK and KR.

(3) drafting of the manuscript; RJ, FDC, FA, RPM, KR

(4) critical revision of the manuscript; MP, MM

(5) approval of the final version of the manuscript; All authors and all authors approved the authorship list.

ABSTRACT

Background: Hepatic stellate cells (HSC) are vital to hepatocellular function and the liver response to injury. They share a phenotypic homology with astrocytes that are central in the pathogenesis of hepatic encephalopathy, a condition in which hyperammonemia plays a pathogenic role. This study tested the hypothesis that ammonia modulates human HSC activation *in vitro* and *in vivo*, and evaluated whether ammonia lowering, by using L-ornithine phenylacetate (OP), modifies HSC activation *in vivo* and reduces portal pressure in a bile duct ligation (BDL) model.

Methods: Primary human HSCs were isolated and cultured. Proliferation (BrdU), metabolic activity (MTS), morphology (TEM, light-and immunofluorescence microscopy), HSC activation markers, ability to contract, and changes in oxidative status (ROS) and endoplasmic reticulum (ER) were evaluated to identify effects of ammonia challenge (50 µM, 100 µM, 300 µM) over 24-72hrs. Changes in plasma ammonia levels, markers of HSC activation, portal pressure and hepatic eNOS activity were quantified in hyperammonemic BDL animals, and after OP treatment.

Results: Pathophysiological ammonia concentrations caused significant and reversible changes in cell proliferation, metabolic activity and activation markers of hHSC *in vitro.* Ammonia also induced significant alterations in cellular morphology, characterised by cytoplasmic vacuolisation, ER enlargement, ROS production, hHSC contraction and changes in pro-inflammatory gene expression together with HSC-related activation markers such as α-SMA, myosin IIa, IIb, and PDGF-Rβ. Treatment with OP significantly reduced plasma ammonia (BDL 199.1µmol/L±43.65 vs. BDL+OP 149.27µmol/L±51.1, P<.05) and portal pressure (BDL 14±0.6 vs. BDL+OP 11±0.3 mmHg, P<.01), which was associated with increased eNOS activity and abrogation of HSC activation markers.

Conclusions: The results show, for the first time, that ammonia produces deleterious morphological and functional effects on HSCs *in vitro*. Targeting ammonia with the ammonia-lowering drug OP reduces portal pressure and deactivates hHSC *in vivo*, highlighting the opportunity for evaluating ammonia lowering as a potential therapy in cirrhotic patients with portal hypertension.

Introduction

Hepatic stellate cells (HSC) orchestrate many important functions in the liver and their activation and consequent dysfunction is associated with many complications including hepatic fibrosis, portal hypertension and liver cancer.[1-3] Astrocytes are cells that are centrally involved in the pathogenesis of hepatic encephalopathy (HE), an important complication of cirrhosis.[4, 5] Hyperammonemia is a feature of liver failure and over the past 120 years many studies have demonstrated incontrovertibly its central role in the pathogenesis of HE.[6, 7] The mechanism of ammonia-induced HE is hypothesised to be through induction of astrocytic osmotic stress swelling induced by glutamine derived from ammonia detoxification by the action of glutamine synthase.[4, 5] More recently, it has been shown that ammonia itself and/or the resulting of cell swelling can initiate a cascade of pathological events such as oxidative stress, resulting in RNA oxidation-and nitrosative stress, leading to nitration of critical proteins.[8] Many studies have indicated that human HSC, like astrocytes share similar markers when activated indicating that they belong to a similar mesodermal origin.[9-12] Both cell types are characterised by a large cytokine repertoire including NFkB-induced pro-inflammatory cytokines.[13-16]

Previous work showed that rat HSCs express glutamine synthetase leading to our hypothesis that excess ammonia may therefore produce deleterious effects on the activity and function of primary human HSC as it does in astrocytes.[17] Following acute or chronic liver injury, HSCs undergo phenotypic transformation from “quiescent” (non-proliferating and non-contractile) to “activated” (promitogenic, profibrogenic, and proinflammatory myofibroblasts-like) cells. Moreover, during the process of activation, HSCs become highly contractile and develop the necessary machinery to contract or relax in response to a number of vasoactive

substances/stimuli.[18-25] Several lines of investigation indicate that activation of HSCs and their ability to contract represent crucial contributory mechanisms associated with the development of portal hypertension, [21, 22, 26] the severity of which has been shown to result in variceal bleeding and a hepatic venous pressure gradient of greater than 10 mmHg is strongly predictive of future decompensation.[27]

The aim of the present study, was to test the hypothesis that ammonia further activates human HSCs (hHSC) *in vitro* and has consequences on hHSC biology. We then tested whether this activation of hHSC occurred *in vivo* by induction of hyperammonemia in a bile duct ligated animal model (BDL). Finally, we tested whether reduction of ammonia by administration of an ammonia-lowering drug L-ornithine phenylacetate (OP) (OCR-002) [28, 29] in BDL rats was associated with a negative modulation of HSC activation and in the reduction of portal pressure.

Materials & Methods

Please refer to the Supplementary Materials and Methods, and Information section for more detailed descriptions.

In vitro studies in human HSC

Primary Human HSCs (hHSC) were isolated from wedge surgical sections of liver normal liver tissue, obtained from patients undergoing surgery in the Royal Free Hospital after giving informed consent (EC01.14-RF). Cells were isolated according to Mederacke et al., [30] with the relative modifications for human liver.[31] Briefly, 10 g of total human liver tissue was digested with 0.01% Collagenase, 0.05% Pronase and 0.001% DNase I without performing perfusion. The homogenate was filtered through a 100µm cell strainer and the flow-through was centrifuged at 50xg for 2 minutes at 4°C. After washing the supernatant, gradient centrifugation was performed at 1400xg for 17 minutes at 4°C using an 11.5% Optiprep gradient. Finally, the interface was collected and washed. Purity of hHSC was established by detection of CD140b (PDGFRbeta), CD29 (Integrin beta 1) and Cytoglobin (CYGB). The obtained HSCs were cultured in RPMI supplemented with 20% foetal bovine serum (FBS), GLUTAMAX, nonessential amino acids 1X, 1.0 mM sodium pyruvate, 1X antibiotic-antimycotic (all Life Technologies), referred to as complete HSC medium hereinafter. Experiments described in this study were performed on hHSC of at least three independent cell preparations between passage 3 and 8.

Treatment: Cells were seeded (density $26x10^3/cm^2$) under basic serum-rich conditions (CM complete medium) for 24 hours, followed by serum deprivation for another 24 hours (SFM). It is well established that ammonia leads to the production of glutamine when GS is present and conversely, glutamine can lead to the

generation of ammonia, not allowing the effects of exogenous ammonia to be studied. Thus, exogenous glutamine was removed from the culture medium to avoid a confounding element in the experimental protocol. Specific treatment with NH_4Cl treatments were replaced daily for the duration of the experiment as described in Supplementary information.

Animal Models

Animals. All animal experiments were conducted according to the Home Office guidelines under the UK Animals in Scientific Procedures Act 1986 with approval of the ethical committee for animal care of University College London. This study was performed in male Sprague-Dawley rats (Charles River UK, Margate, UK), weighing 220–250 g.

In one experimental model, rats were administered a high protein/ammoniagenic diet (AAs) for 5 days.[13, 32] Furthermore, all rats underwent BDL to induce cirrhosis or a sham operation as described previously.[33]

Study design. (i) In this experimental protocol, animals underwent BDL surgery and were given 4 weeks to develop liver injury. During the 4th week, BDL animals were randomized into 3 groups: one group included BDL rats receiving an amino acid-rich (AAs) diet in addition to injection of intraperitoneal (i.p.) saline solution (n=4); a second group received the AAs diet and was treated with an i.p. injection of the ammonia-lowering agent OP 0.3 g/kg twice a day for 5 days (n=4); the third group consisted of BDL rats receiving saline solution i.p. (n=4). In addition to the BDL animals, a further group of sham-operated rats received saline solution (i.p.) (n=4). Animals were sacrificed on the 5th day of treatment.

(ii) In a second experimental protocol, the effect of the ammonia-lowering agent OP on ammonia-induced portal hypertension was investigated. Four weeks after BDL or sham operation, rats were randomized into three groups: sham-operated rats receiving saline (i.p.) (n=18) twice a day for the experimental period of 5 days; BDL rats (n=20) were administered i.p. saline twice a day for 5 days; a further group of BDL rats (n=11) received i.p. injection of OP 0.3 g/kg twice a day for 5 days. Between weeks 4 and 5, following anesthesia (2% isofluorane), rats from each group underwent assessment of mean arterial pressure via isolation and cannulation of the right carotid artery. In addition, portal pressure was measured by direct cannulation of the main portal vein. All measurements were transduced to a Powerlab (4SP) linked to Chart v5.0.1 software. The mean of three readings taken one minute apart was recorded. Liver tissue was harvested and snap-frozen for storage at 80°C until analyzed.

Statistical analysis

Results are expressed as mean values ± SEM and compared using one-way analysis of variance followed by Dunnet's or Tukey's multiple comparison post hoc tests, where appropriate. *P* values ≤0.05 were considered significant.

In vivo experimental data were analysed by t tests and Mann-Whitney U test as appropriate; *P* <0.05 was considered statistically significant. Results are presented as mean values ± SEM using GraphPad Prism software (GraphPad, La Jolla, CA).

Results

Ammonia reduces cell proliferation and metabolism in human Hepatic Stellate Cells in vitro in a dose dependent manner

Human HSC treated with different concentrations of ammonia for 72 hours showed a significant inhibition in cell proliferation (BrdU assay) and metabolic activity (MTS assay) (**Fig. 1A**). Furthermore, long term treatment of hHSC with ammonia did not cause cell death as assessed by deploying the Cell Death Detection ELISA (**Fig. 1B**). Also, these ammonia-induced effects coincided with strong alterations in cellular morphology in a dose-dependent manner as observed by light microscopy (**Fig. 1C**). Treatment with ammonia led to drastic changes in cell morphology with the appearance of a spindle-like fibroblast phenotype, and signs of deregulation of the endo-lysosomal compartment as assessed by Neutral Red, a dye retained by the lysosomes (**Fig. 1C**). As demonstrated in Supplementary Fig.1 human HSC express GS at the mRNA and protein level. Pretreatment of cells with MSO, a biochemical inhibitor of GS, followed by exposure to ammonia did not further inhibit proliferation and metabolic activity in comparison to MSO treatment only (**Supplementary Fig. 1**).

Ammonia induces alterations in cytoplasmic stress, which coincides with changes in cellular metabolism/function and actin cytoskeleton architecture

The morphological changes observed by light microscopy were further characterised by performing ultrastructural studies. Ammonia caused a dramatic dose-dependent change in the cytosol with ER enlargement and marked presence of translucent vacuoles. Neither mitochondrial alterations nor presence of autophagic structures (characterised by double membranes) were observed (**Fig. 2A**). Of importance is the

fact that when ammonia-rich medium was removed and cells were replenished with complete medium both cell proliferation and metabolic activity were restored (**Fig. 2B**), thus supporting the idea that the observed effect of ammonia is transient. Moreover, ammonia-treated hHSC cultured on collagen gels showed a significant ability to contract (**Fig. 2C, 2D**) when compared to control. This effect was observed as soon as three hours of ammonia treatment and appeared to be still sustained after 24 hours which coincided with the previously observed morphological changes (**Fig. 2E**). Furthermore, long-term treatment with ammonia (72 hours) induced a dose-dependent re-organization of filamentous actin in the cytoskeleton when TRICT-Phalloidin staining was employed. Re-organization of the F-actin network coincided with the presence of translucent vacuoles in a dose depended manner (**Fig. 2F**).

Ammonia induces ER enlargement

As the ultrastructural study showed a marked ammonia-dependent dysregulation and enlargement of the ER compartment, we then further evaluated the status of ER stress. To this end, cells were cultured and treated with ammonia as previously described, for 1, 3 up to 24 hours, followed by qPCR for two ER stress marker genes i.e. ATF6 and XBP1. Both, mRNA expression levels were up-regulated in a dose-and time dependent manner with a marked up-regulation after 3 hours for all ammonia concentrations tested, which decreased again after 24 hours of treatment (**Fig. 3A**). Moreover, pre-treatment with TUDCA, a bile salt derivate with ER-chaperone properties, alleviated the previously shown increase in ammonia-induced ATF6 and XBP1 mRNA expression after 3 hours. Prolonged treatment with ammonia for 72 hours, altered the ER dynamics with a strong peri-nuclear accumulation of ER-

Tracker™ Red dye and the presence of cytoplasmic vacuoles with increasing ammonia concentrations (**Fig. 3C**).

Hyperammonemia induces ROS production in hHSC

As ER stress is associated with or/and leads to ROS formation, the possibility that ammonia stimulates ROS production was assessed. Prolonged treatment of cells with ammonia for up to 72 hours showed a gradual development of ROS as detected by the presence of cytosolic carboxy-DCF (**Fig. 4A**). The development of ammonia-induced ROS production was further quantitatively measured as described previously,[34] and confirmed that primary hHSCs treated with ammonia produced significant ROS (**Fig. 4B**). Next, cells treated with ammonia for different time points showed a strong increase in mRNA expression of Superoxide dismutase 2 (SOD2) after 3 hours, which was sustained at 24 hours of ammonia treatment (**Fig. 4C**). Moreover, pre-treatment with N-acetyl cysteine (NAC), a known ROS scavenger, showed no impact on the previously observed increase in SOD2 mRNA expression after 3 hours of ammonia treatment. In contrast, pre-treatment with NAC followed by ammonia treatment for 24 hours, almost completely abolished ammonia-induced SOD2 mRNA expression.

Ammonia alters the pro-fibrogenic/pro-inflammatory profile in hHSC

Next, the possibility that ammonia-induced ROS formation causes alterations in HSC-related activation markers and pro-inflammatory genes was investigated. As shown in **Fig. 5A**, ammonia was shown to significantly increase α-SMA protein expression. At 300μM ammonia, vimentin (an important intermediate filament) synthesis was increased. Both Myosin IIa (that plays a key role in HSC contraction)

and Myosin IIb (implicated in HSC activation), were significantly modulated by increasing concentrations of ammonia. A dose-dependent response to ammonia was also observed in P-38 MAPK expression. Furthermore, PDGFR-β, important in HSC cell proliferation, showed a significant up-regulation under influence of ammonia, whereas Collagen type I showed a tendency to increase by ammonia, albeit these effects were not statistically significant (**Fig. 5A**). Furthermore, ammonia induced a strong and significant up-regulation of MMP2 mRNA expression, whereas mRNA expression of TIMP1 was down-regulated (**Fig. 5B**). Moreover, pro-inflammatory Interleukin-1β mRNA expression was significantly induced when hHSC were treated with ammonia 300 µM for 72 hours (**Fig. 5C**), whereas ammonia at 50 µM and 100 µM doses significantly up-regulated Interleukin 6 mRNA expression level. By contrast, ammonia did not modify Interleukin 8 mRNA expression in HSC (**Fig. 5C**).

In vivo study I: Bile duct ligation and ammonia treatment modifies HSC cell biology in vivo

In a first set of *in vivo* experiments the effect of hyperammonemia on HSC-related signalling pathways in whole liver tissue was investigated. As previously described[13] ammonia concentrations were noted to be significantly elevated in BDL rat plasma compared to sham-operated rats (149.3µmol/L±51.1 vs. 107.4µmol/L±23.2, $P < .05$). Plasma ammonia levels further increased when animals were fed an amino acid-rich (AAs) diet in combination with BDL surgery (199.1µmol/L±43.6 vs. 149.3µmol/L±51.1, $P < .05$) (**Fig. 6A**). More importantly, plasma ammonia levels decreased significantly when BDL-AAs-fed animals were treated with OP (123.9µmol/L±16.1 vs.199.1µmol/L µM±43.6, $P < .001$) (**Fig. 6A**). These significant changes in ammonia plasma levels were correlated with alterations

in portal pressure which was significantly higher in BDL rats and BDL-AAs-fed animals compared to sham (**Supplementary Fig. 2**). Expectedly, as the animals in the OP group were only treated for 5-days, no differences in collagen accumulation, assessed by Picrosirius Red staining, was demonstrated between BDL–AAs-fed animals and BDL–AAs-fed OP treated animals (**Supplementary Fig. 3**).

Of note, the observed changes in haemodynamics post OP treatment coincided with a marked decrease in protein expression of HSC-related activation markers (**Fig. 6B**). More specifically, BDL in combination with hyperammonaemia (AAs diet) showed a significant increase in Myosin IIb, Collagen type I, and PDGF-Rβ protein expression in comparison to BDL. In contrast, treatment with OP abrogated the strong effect of hyperammonaemia on BDL rat livers in relation to all HSC-related activation markers tested (**Fig. 6B**).

As ammonia-induced ER enlargement in hHSCs *in vitro* (**Fig. 3A**) the expression of ER stress-markers (CHOP and BiP) was evaluated *in vivo*. CHOP protein expression was increased in BDL and BDL-AAs-fed animals in comparison to sham-operated animals, with a minor but significant down regulation in BDL–AAs-fed and OP-treated animals (Fig. 6C). In contrast, BiP protein expression was significantly down regulated in all BDL treated animals in comparison to Sham-operated rats, whereas OP treatment significantly prevented BiP protein down regulation in comparison to BDL–AAs-fed animals (**Fig. 6C**). Overall, these data indicate that OP treatment abolishes ammonia-induced ER-stress, with associated reduced HSC activation and consequent reduction in portal pressure.

In vivo study II: Treatment with OP improves portal pressure through reduction in nitrosative stress

As described above, in the second *in vivo* study, ammonia concentrations were noted to be significantly elevated in BDL rat plasma compared to sham-operated rats (182±12.8 vs. 62.51±6.2 μM, $P < .0001$), and this decreased significantly following treatment with OP (83.8±16.3 μM, $P < .0001$). These significant changes in plasma ammonia were correlated with alterations in portal pressure, which was significantly higher in BDL rats compared to sham (14±0.6 vs.5.5±0.3 mmHg, $P < .0001$) (**Fig. 7A**). Ammonia lowering through administration of OP resulted in a significant reduction in portal pressure compared to BDL –saline treated rats (11±0.3 mmHg, $P < .01$). Mean arterial pressure (MAP) was significantly higher in sham rats compared with BDL animals (105±2.3 vs 80±2.9 mmHg, $P < .001$). Following OP therapy, there was no significant change in MAP observed between BDL saline and OP treated rats (**Fig. 7A**). As a consequence of the ammonia-induced inflammatory and oxidative pathways observed in HSCs *in vitro*, and the effect of hyperammonemia on HSC-related activation markers *in vivo*, the impacts on nitrosative stress was also assessed in whole liver tissue. When compared to sham-operated rats, there were significant increases in iNOS protein expression in BDL rats (**Fig. 7B**). Treatment with OP significantly reduced iNOS expression when compared to BDL control animals. Moreover, 3-NTyrosine expression (as an indication of increased nitrosative stress), was also significantly up-regulated in BDL treated animals compared to sham animals and this was reduced significantly following treatment with OP (**Fig. 7C**). eNOS protein expression was significantly increased in BDL rats compared to sham animals (as we previously described[34]) and this remained statistically unchanged after OP therapy (**Fig. 7C**). More importantly, a significant reduced eNOS enzyme activity was observed in BDL rat liver compared to sham-operated animals, which was restored to near normal levels after OP therapy. Furthermore, the

expression of Caveolin-1 (an intracellular eNOS inhibitor) was found to be significantly higher in BDL livers compared to sham rats. In contrast, in BDL animals treated with OP, Caveolin-1 expression showed a significant down regulation in comparison to BDL rats (**Fig. 7C**).

Discussion

The results of this study reveal, for the first time, that pathophysiologically relevant concentrations of ammonia produce marked deleterious consequences on HSCs *in vitro* and *in vivo* including: changes in endoplasmic reticulum dynamics and increase cellular oxidative stress, which are transient and can be prevented by intervention, providing therapeutic opportunities. Reduction in ammonia concentration using the ammonia-lowering drug OP, for a short term treatment of 5 days, resulted in a down regulation of HSCs activation markers in BDL rats that coincided with a significant reduction in portal pressure, providing a potential novel strategy to treat portal hypertension.

The first set of experiments clearly showed that increasing concentrations of ammonia were associated with marked structural and functional changes of hHSCs. This was not associated with any evidence of cell-death and notably these effects were reversible when ammonia was removed from the medium and cells were allowed to recover. Hence, providing the first indication that ammonia-induced dysfunction of HSCs is reversible. In accordance with prior observations in rat HSCs[17], human HSCs also express GS. Interestingly, although GS gene expression remained unaffected by increasing concentrations of ammonia, a significant reduction in protein levels was observed. The mechanism(s) of this reduction is not clear but may be a consequence of reduced detection or breakdown, as ammonia has been shown to nitrosylate GS in astrocytes.[35-37]

These changes in functionality as observed in this study were closely associated with dose-dependent morphological alterations, as assessed by light and transmission electron microscopy. On light microscopy, cells appeared longer, spindly and also presented marked vacuolization. These alterations were further

confirmed by ultra-structural analysis as evidenced by dose-dependent cytoplasmic vacuolization, with no significant nuclear alterations. Whilst the treatment of astrocytes with ammonia has been shown to induce mitochondrial swelling [38] and autophagy, in this study, ammonia induced cytoplasmic vacuolization in hHSCs was without the formation of autophagic bodies or alterations in mitochondrial structure. Indeed, ammonia-induced autophagy has been shown to be cell type and context dependent.[39, 40] These morphological changes coincided with modifications in the actin cytoskeletal architecture such as the re-organization in filamentous actin and a significant up-regulation in α-SMA and myosin IIa protein expression, after a prolonged treatment with ammonia. Furthermore, ammonia induced contraction of hHSC, indicating that ammonia strongly affects actin, which is important in maintaining HSC cell integrity and function.

In this study, evidence of marked ER swelling and vacuolisation was observed. The ER uses its protein folding status as a signal to orchestrate downstream apoptotic or adaptive responses and the ER is known as a key player in the process of liver damage.[41] Moreover, it is known that ER stress can induce activation of primary hHSC and induce its morphological changes and dysfunction through induction of autophagy.[42] In this study, ammonia induced, in a time dependent manner, ER stress markers, which coincided with up-regulation of HSC activation markers but without affecting apoptosis and autophagy. Moreover, the co-involvement of ammonia-induced ER stress in hHSC was further demonstrated by using Tauroursodeoxycholic Acid (TUDCA) [40] known to exert protection from liver injury by inhibiting ER-stress.

In order to determine the effectors of these functional and morphological changes induced by ammonia, our study further focused on the development of oxidative

stress. It was remarkable to note that the hHSC were very sensitive to ammonia in inducing intracellular production of reactive oxygen species as assessed by a quantitative fluorometric assay. The mechanisms of this increase in ROS with ammonia are not entirely clear but are thought to be consequent upon ER enlargement and cell swelling and/or generation of cytokines as shown in this study. Indeed, the co-involvement of ammonia-induced ER-stress followed by ROS formation in hHSC was further demonstrated by using TUDCA and NAC, inhibitors of ER stress and scavenger of ROS respectively. Moreover, this increase in oxidative stress can have deleterious consequences on chronic activation of wound healing.[43] Similar results are well established for the role of ROS production in portal hypertension, that result in a paracrine activation and proliferation of hepatic sinusoidal endothelial cells, which in turn will activate HSCs resulting in their proliferation, migration, contraction and further fibrogenesis.[44-46] The cross talk between HSCs and LSEC needs further investigation, as this complex interaction, may be impacted upon by reduction in ammonia concentrations.

Overall, the ammonia-induced ROS production affects the mRNA and protein expression levels of HSC activation markers and several pro-inflammatory interleukins. It was therefore notable that the protein expression for p38MAP kinase was increased by ammonia in the hHSC, which is a key signal transduction mediator of inflammation in many cell types.[47] Previous studies have indicated a similar up-regulation of gene and protein expression of p38MAP kinase in astrocytes and also in neutrophils after exposure to ammonia. In fact, inhibition of p38MAP kinase in neutrophils reversed this ammonia-induced functional derangement.[32, 48, 49]

In order to determine whether this observation *in vitro* could be translated *in vivo*, we chose to study BDL animals that are spontaneously mildly hyperammonemic.

Further exaggeration of hyperammonemia in these animals using a hyperammonemic diet resulted in an additional increased protein expression of HSC activation markers such as Myosin IIa and IIb, αSMA, PDFRβ and Collagen-1. These HSC markers were significantly reduced following treatment with OP, an ammonia lowering drug which has previously been shown to lower plasma ammonia concentrations.[28] These data provide direct *in vivo* evidence that hyperammonemia induces HSC activation and that lowering ammonia concentration reduces this activation.

In order to test whether ammonia reduction is a target for the treatment of portal hypertension, we chose to study the BDL animal model, which is known to exhibit hyperammonemia, increased portal pressure and is clinically relevant.[28] In this model, the effect of ammonia reduction on eNOS activity in the brain was previously investigated using OP. The results showed reduction in brain water and improved brain eNOS activity through effects upon eNOS regulators.[50] The same model was used in this study to examine the effect of OP on portal pressure. Reduction in ammonia with OP was associated with a significant and marked reduction in portal pressure to values that were not significantly different to control animals without any significant change in the mean arterial pressure. This improvement in portal pressure was associated with a reduction in markers of oxidative and nitrosative stress such as iNOS and 5-nitrotyrosine, and induction in eNOS enzyme activity.

In conclusion, the data presented in this paper provide the first indication that ammonia affects HSCs cell behaviour by changing ER dynamics and producing oxidative stress that result in HSC activation, and functional and morphological disturbances. This leads to the generation of many pro-inflammatory, contractile and pro-fibrogenic genes and proteins *in vitro* and *in vivo.* Importantly, by removal of

ammonia *in vitro*, or by lowering ammonia *in vivo*, HSC biology is restored. Indeed, reduction in ammonia concentration in a clinically relevant rat model of cirrhosis using OP (OCR-002), a drug in development for treatment of hyperammonemia and HE, resulted in a downregulation of HSCs activation markers, which coincided with a reduction in severity of many important pathophysiological determinants of portal hypertension. This suggests that ammonia is a possible target for therapy and justifies a clinical trial of ammonia lowering in portal hypertension.

FIGURE LEGENDS

Fig. 1. Ammonia reduces in a dose dependent manner cell proliferation and metabolism in primary human Hepatic Stellate Cells *in vitro.* (A) Ammonia inhibits DNA synthesis (BrdU) and metabolic activity (MTS), (B) without inducing cell death. (C) Ammonia induced strong morphological changes in a dose-dependent manner i.e. from myofibroblast-like cells into spindle like fibroblasts as was observed by light microscopy and by Neutral Red cell viability test (20X, 40X). Bar graphs show means of three independent values ± SD. **P* < .05, ***P* < .01 and ****P* < .001 *vs.* corresponding values of serum free medium (SFM).

Fig. 2. Ammonia induces alterations in cytoplasmic stress, which coincides with changes in cellular metabolism/function, contraction and actin cytoskeleton architecture.

(A) Transmission Electron Microscopy (TEM) shows that ammonia in a dose-dependent manner caused dramatic morphological changes with appearance of cytoplasmic vacuoles (V=vacuoles; N=nucleus). (B) Recovery of cell proliferation after depletion of ammonia-rich culture medium. Bar graphs show means of three independent values ± SD. **P* < .05 and ****P* < .001 vs. SFM. (C, D) Collagen gel contraction assay shows that ammonia induces hHSC contraction. Bar graphs show means of 2 independent experiments (values ± SD. *P < .05 and **P < .01 vs. corresponding values of SFM. (E) Ammonia-induced HSC contraction coincides with changes in morphology. (F) Prolonged treatment (72h) with ammonia induces in a dose-dependent manner the re-organization of filamentous actin (TRITC-Phalloidin staining).

Fig. 3. Ammonia induces ER-stress.

(A) Ammonia affects mRNA expression levels of ER stress markers ATF6 and XBP1 in a dose and time-dependent manner. Bar graphs show means of 2 independent values ± SD. ***P < .001 vs corresponding values of SFM. (B) Pretreatment of hHSC with TUDCA, a chemical chaperone of ER stress, abrogates ammonia-induced ATF6 and XBP1 mRNA expression. Bar graphs show means of 2 independent values ± SD. *P < .05 **P < .01 vs corresponding values of SFM. (C) Prolonged treatment of cells with ammonia for 72 hours induces ER-enlargement in hHSC. Changes in ER dynamics are observed by ER-Tracker™ Red.

Fig. 4. Ammonia induces ROS production.

(A) Prolonged treatment of hHSC with ammonia for 72 hours induces ROS production in hHSC. The formation of reactive oxygen species (ROS) was measured using Image-IT™ LIVE Green Reactive Oxygen Species Detection Kit. (B) Mean fluorescence intensity (MFI) of ROS signal was normalized according to the number of cells (Hoechst 33342), and expressed as percentage of control. Bar graphs show means of three independent values ± SD. ***P < .001 vs corresponding values of SFM. (C) Hyperammonemia increases mRNA expression level of ROS marker SOD2 at 3 and 24 hours. Bar graphs show means of 2 independent values ± SD. ***P < .001 vs corresponding values of SFM. (D) NAC-induced ROS scavenger reduces ammonia-induced SOD2 mRNA expression at 24 hours. Bar graphs show means of 2 independent values ± SD. *P < .05 **P < .01 vs corresponding values of SFM.

Fig. 5. Ammonia modifies mRNA expression and protein level of several pro-inflammatory and HSC activation markers.

(A) Ammonia affects protein expression of α-SMA, vimentin, PDGF-Rβ, Myosin IIa and IIb, and p-38 MAPK. (B) Ammonia induces up-regulation of MMP2 mRNA whereas TIMP1 mRNA is down-regulated, and (C) Interleukin 1β and Interleukin IL6 mRNA expression are upregulated. Bar graphs show means of three independent values ± SD. **P* < .05, ***P* < .01 and ****P* < .001 vs. corresponding values of SFM.

Fig. 6. Hyperammonemia treatment further enhances BDL-induced HSC markers *in vivo*.

(A) Plasma levels of ammonia are significant upregulated in BDL and AAs-fed BDL animals in comparison to sham operated rats (**P* < .05 and ***P* < .01 vs Sham). OP treatment reduces significant ammonia in BDL-AAs-fed animals in comparison to BDL animals (***P* < .01). (B) Hyperammonemia treatment in BDL-induced fibrosis showed an additional significant increase in Myosin IIb, Collagen type I and PDGF-Rβ protein expression in comparison to BDL-induced fibrosis (***P* < .01 and ****P* < .001). In contrast, treatment with OP, abrogated the strong effect of AAs-fed BDL on all HSC-related activation markers (**P* < .05, ***P* < .01 and ****P* < .001). (C) CHOP protein expression was increased in BDL and BDL-AAs-fed animals with a minor but significant down regulation in BDL–AAs-OP-treated animals (**P* < .05 vs BDL -AAs-fed). BiP protein expression was significantly down regulated in all BDL treated animals in comparison to Sham-operated rats, whereas OP treatment significantly prevented BiP protein down regulation in comparison to BDL–AAs-fed animals (**P* < .05 vs BDL -AAs-fed).

Fig. 7. Treatment with OP improves portal pressure through reduction in nitrosative stress. (A) Portal pressure show to be increased in BDL rats compared to sham (***P < .001). Administration of OP results in a significant lowering of portal pressure compared to BDL–saline treated rats (**P < .01). Mean arterial pressure (MAP) was significantly higher in sham rats compared with BDL animals (**P < .01) with no change observed between BDL and OP treated rats (NS). (B) iNOS protein expression in BDL rats significantly increases when compared to sham animals (***P < .001), whereas treatment with OP significantly reduces iNOS expression when compared to BDL animals (**P < .01). 3-NTyrosine expression was significantly up-regulated in BDL treated animals compared to sham and this was reduced significantly following treatment with OP (**P< .01 vs. Sham, *P < .05 vs. BDL). (C) Protein expression of eNOS was significantly increased in BDL rats compared to sham animals (***P < .001) and remained unchanged after OP therapy. A significant reduced eNOS activity was observed in BDL rats compared to sham-operated animals (*P < .05) and this was restored to near normal levels after OP therapy (*P < .05 vs BDL). Caveolin-1 expression was upregulated in BDL livers compared to sham rats (***P < .001) and was downregulated upon with OP treatment (**P < .01 vs. BDL).

References

[1]Friedman SL. Hepatic stellate cells: protean, multifunctional, and enigmatic cells of the liver. Physiol Rev 2008;88:125-172.

[2]Schuppan D, Kim YO. Evolving therapies for liver fibrosis. J Clin Invest 2013;123:1887-1901.

[3]Pinzani M, Rombouts K. Liver fibrosis: from the bench to clinical targets. Dig Liver Dis 2004;36:231-242.

[4]Martinez-Hernandez A, Bell KP, Norenberg MD. Glutamine synthetase: glial localization in brain. Science 1977;195:1356-1358.

[5]Haussinger D, Schliess F. Pathogenetic mechanisms of hepatic encephalopathy. Gut 2008;57:1156-1165.

[6]Shawcross DL, Olde Damink SW, Butterworth RF, Jalan R. Ammonia and hepatic encephalopathy: the more things change, the more they remain the same. Metabolic brain disease 2005;20:169-179.

[7]Olde Damink SW, Deutz NE, Dejong CH, Soeters PB, Jalan R. Interorgan ammonia metabolism in liver failure. Neurochemistry international 2002;41:177-188.

[8]**Gorg B, Qvartskhava N,** Keitel V, Bidmon HJ, Selbach O, Schliess F, et al. Ammonia induces RNA oxidation in cultured astrocytes and brain in vivo. Hepatology 2008;48:567-579.

[9]Geerts A. History, heterogeneity, developmental biology, and functions of quiescent hepatic stellate cells. Semin Liver Dis 2001;21:311-335.

[10]Niki T, De Bleser PJ, Xu G, Van den Berg K, Wisse E, Geerts A. Comparison of glial fibrillary acidic protein and desmin staining in normal and CCl4-induced fibrotic rat livers. Hepatology 1996;23:1538-1545.

[11]Geerts A, Eliasson C, Niki T, Wielant A, Vaeyens F, Pekny M. Formation of normal desmin intermediate filaments in mouse hepatic stellate cells requires vimentin. Hepatology 2001;33:177-188.

[12]Albert G, Pekny M. Hepatic stellate cells and astrocytes: similarities and differences. In Hepatic Enchephalopathy and Nitrogen Metabolism, 87-111, SPRINGER; 2006.

[13]**Wright G, Davies NA,** Shawcross DL, Hodges SJ, Zwingmann C, Brooks HF, et al. Endotoxemia produces coma and brain swelling in bile duct ligated rats. Hepatology 2007;45:1517-1526.

[14]**Wright GA, Sharifi Y,** Newman TA, Davies N, Vairappan B, Perry HV, et al. Characterisation of temporal microglia and astrocyte immune responses in bile duct-ligated rat models of cirrhosis. Liver international 2014;34:1184-1191.

[15]Bataller R, Brenner DA. Liver fibrosis. J Clin Invest 2005;115:209-218.

[16]Hernandez-Gea V, Friedman SL. Pathogenesis of liver fibrosis. Annu Rev Pathol 2011;6:425-456.

[17]Bode JG, Peters-Regehr T, Gressner AM, Haussinger D. De novo expression of glutamine synthetase during transformation of hepatic stellate cells into myofibroblast-like cells. The Biochemical journal 1998;335 (Pt 3):697-700.

[18]Pinzani M, Failli P, Ruocco C, Casini A, Milani S, Baldi E, et al. Fat-storing cells as liver-specific pericytes. Spatial dynamics of agonist-stimulated intracellular calcium transients. J Clin Invest 1992;90:642-646.

[19]Kawada N, Klein H, Decker K. Eicosanoid-mediated contractility of hepatic stellate cells. The Biochemical journal 1992;285 (Pt 2):367-371.

[20]Rockey DC, Housset CN, Friedman SL. Activation-dependent contractility of rat hepatic lipocytes in culture and in vivo. J Clin Invest 1993;92:1795-1804.

[21]Reynaert H, Thompson MG, Thomas T, Geerts A. Hepatic stellate cells: role in microcirculation and pathophysiology of portal hypertension. Gut 2002;50:571-581.

[22]Reynaert H, Urbain D, Geerts A. Regulation of sinusoidal perfusion in portal hypertension. Anat Rec (Hoboken) 2008;291:693-698.

[23]**Liu Z, van Grunsven LA,** Van RE, Schroyen B, Timmermans JP, Geerts A, et al. Blebbistatin inhibits contraction and accelerates migration in mouse hepatic stellate cells. Br J Pharmacol 2010;159:304-315.

[24]Vanheule E, Geerts AM, Reynaert H, Van VH, Geerts A, De VM, et al. Influence of somatostatin and octreotide on liver microcirculation in an experimental mouse model of cirrhosis studied by intravital fluorescence microscopy. Liver Int 2008;28:107-116.

[25]Liu Z, Van RE, Timmermans JP, Geerts A, van Grunsven LA, Reynaert H. Distinct roles for non-muscle myosin II isoforms in mouse hepatic stellate cells. J Hepatol 2011;54:132-141.

[26]Geerts A, Timmermans JP, Reynaert H. Hepatic circulation. Anat Rec (Hoboken) 2008;291:611-613.

[27]Bosch J, Abraldes JG, Berzigotti A, Garcia-Pagan JC. The clinical use of HVPG measurements in chronic liver disease. Nature reviews Gastroenterology & hepatology 2009;6:573-582.

[28]**Davies NA, Wright G,** Ytrebo LM, Stadlbauer V, Fuskevag OM, Zwingmann C, et al. L-ornithine and phenylacetate synergistically produce sustained reduction in ammonia and brain water in cirrhotic rats. Hepatology 2009;50:155-164.

[29]Ytrebo LM, Kristiansen RG, Maehre H, Fuskevag OM, Kalstad T, Revhaug A, et al. L-ornithine phenylacetate attenuates increased arterial and extracellular brain

ammonia and prevents intracranial hypertension in pigs with acute liver failure. Hepatology 2009;50:165-174.

[30]**Mederacke I, Dapito DH,** Affo S, Uchinami H, Schwabe RF. High-yield and high-purity isolation of hepatic stellate cells from normal and fibrotic mouse livers. Nature protocols 2015;10:305-315.

[31]Rombouts K, Carloni V. Determination and characterization of tetraspanin-associated phosphoinositide-4 kinases in primary and neoplastic liver cells. In: Waugh MG, editor. Lipid Signaling Protocols, 2 ed. New York: Springer Science+Business Media; 2015. p. 203-212.

[32]Shawcross DL, Wright GA, Stadlbauer V, Hodges SJ, Davies NA, Wheeler-Jones C, et al. Ammonia impairs neutrophil phagocytic function in liver disease. Hepatology 2008;48:1202-1212.

[33]Harry D, Anand R, Holt S, Davies S, Marley R, Fernando B, et al. Increased sensitivity to endotoxemia in the bile duct-ligated cirrhotic Rat. Hepatology 1999;30:1198-1205.

[34]Mookerjee RP, Wiesenthal A, Icking A, Hodges SJ, Davies NA, Schilling K, et al. Increased gene and protein expression of the novel eNOS regulatory protein NOSTRIN and a variant in alcoholic hepatitis. Gastroenterology 2007;132:2533-2541.

[35]Gorg B, Wettstein M, Metzger S, Schliess F, Haussinger D. LPS-induced tyrosine nitration of hepatic glutamine synthetase. Hepatology 2005;42:499.

[36]Schliess F, Gorg B, Fischer R, Desjardins P, Bidmon HJ, Herrmann A, et al. Ammonia induces MK-801-sensitive nitration and phosphorylation of protein tyrosine residues in rat astrocytes. FASEB journal : 2002;16:739-741.

[37]Haussinger D, Gorg B, Reinehr R, Schliess F. Protein tyrosine nitration in hyperammonemia and hepatic encephalopathy. Metabolic brain disease 2005;20:285-294.

[38]Gregorios JB, Mozes LW, Norenberg MD. Morphologic effects of ammonia on primary astrocyte cultures. II. Electron microscopic studies. Journal of neuropathology and experimental neurology 1985;44:404-414.

[39]Sun R, Luo Y, Li J, Wang Q, Li J, Chen X, et al. Ammonium chloride inhibits autophagy of hepatocellular carcinoma cells through SMAD2 signaling. Tumour biology : the journal of the International Society for Oncodevelopmental Biology and Medicine 2015;36:1173-1177.

[40]Li X, Wang Y, Wang H, Huang C, Huang Y, Li J. Endoplasmic reticulum stress is the crossroads of autophagy, inflammation, and apoptosis signaling pathways and participates in liver fibrosis. Inflammation research : official journal of the European Histamine Research Society [et al] 2015;64:1-7.

[41]Hernandez-Gea V, Hilscher M, Rozenfeld R, Lim MP, Nieto N, Werner S, et al. Endoplasmic reticulum stress induces fibrogenic activity in hepatic stellate cells through autophagy. J Hepatol 2013;59:98-104.

[42]Xie Q, Khaoustov VI, Chung CC, Sohn J, Krishnan B, Lewis DE, et al. Effect of tauroursodeoxycholic acid on endoplasmic reticulum stress-induced caspase-12 activation. Hepatology 2002;36:592-601.

[43]Novo E, Cannito S, Paternostro C, Bocca C, Miglietta A, Parola M. Cellular and molecular mechanisms in liver fibrogenesis. Arch Biochem Biophys 2014;548:20-37.

[44]Gracia-Sancho J, Maeso-Diaz R, Fernandez-Iglesias A, Navarro-Zornoza M, Bosch J. New cellular and molecular targets for the treatment of portal hypertension. Hepatology international 2015;9:183-191.

[45]**Urtasun R, Conde de la Rosa L,** Nieto N. Oxidative and nitrosative stress and fibrogenic response. Clinics in liver disease 2008;12:769-790, viii.

[46]Sanchez-Valle V, Chavez-Tapia NC, Uribe M, Mendez-Sanchez N. Role of oxidative stress and molecular changes in liver fibrosis: a review. Current medicinal chemistry 2012;19:4850-4860.

[47]Zarubin T, Han J. Activation and signaling of the p38 MAP kinase pathway. Cell research 2005;15:11-18.

[48]Panickar KS, Jayakumar AR, Rao KV, Norenberg MD. Ammonia-induced activation of p53 in cultured astrocytes: role in cell swelling and glutamate uptake. Neurochemistry international 2009;55:98-105.

[49]Agusti A, Cauli O, Rodrigo R, Llansola M, Hernandez-Rabaza V, Felipo V. p38 MAP kinase is a therapeutic target for hepatic encephalopathy in rats with portacaval shunts. Gut 2011;60:1572-1579.

[50]**Balasubramaniyan V, Wright G,** Sharma V, Davies NA, Sharifi Y, Habtesion A, et al. Ammonia reduction with ornithine phenylacetate restores brain eNOS activity via the DDAH-ADMA pathway in bile duct-ligated cirrhotic rats. American journal of physiology Gastrointestinal and liver physiology 2012;302:G145-152.

"Author names in bold designate shared co-first authorship"

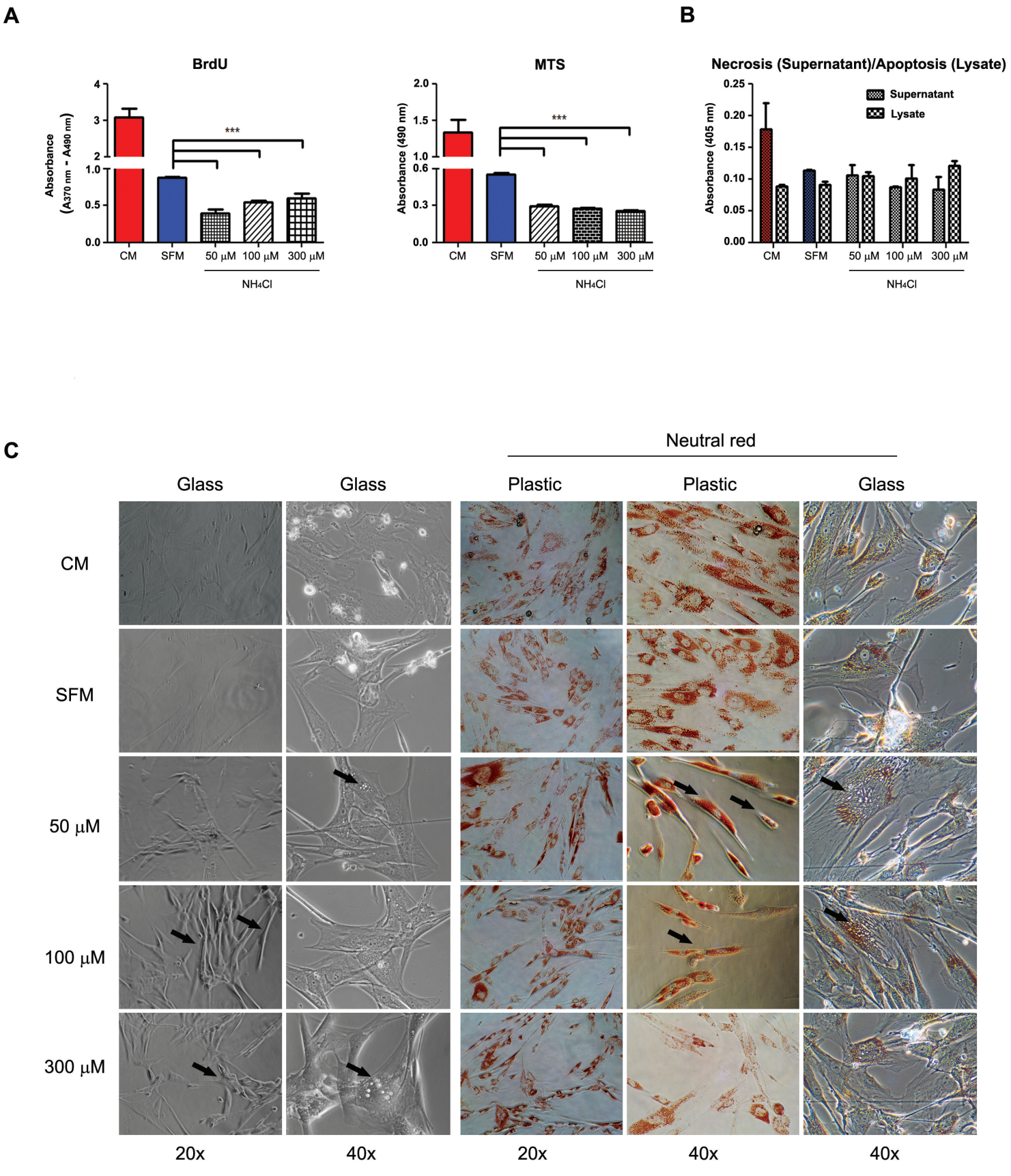
A
BrdU
Absorbance (A370 nm - A490 nm)
4
3
2
1.0
0.5
0.0
***
CM
SFM
50 µM
100 µM
300 µM
NH4Cl
MTS
Absorbance (490 nm)
2.0
1.5
1.0
0.6
0.3
0.0
***
CM
SFM
50 µM
100 µM
300 µM
NH4Cl
B
Necrosis (Supernatant)/Apoptosis (Lysate)
Absorbance (405 nm)
0.25
0.20
0.15
0.10
0.05
0.00
Supernatant
Lysate
CM
SFM
50 µM
100 µM
300 µM
NH4Cl
C
Neutral red
Glass
Glass
Plastic
Plastic
Glass
CM
SFM
50 µM
100 µM
300 µM
20x
40x
20x
40x
40x

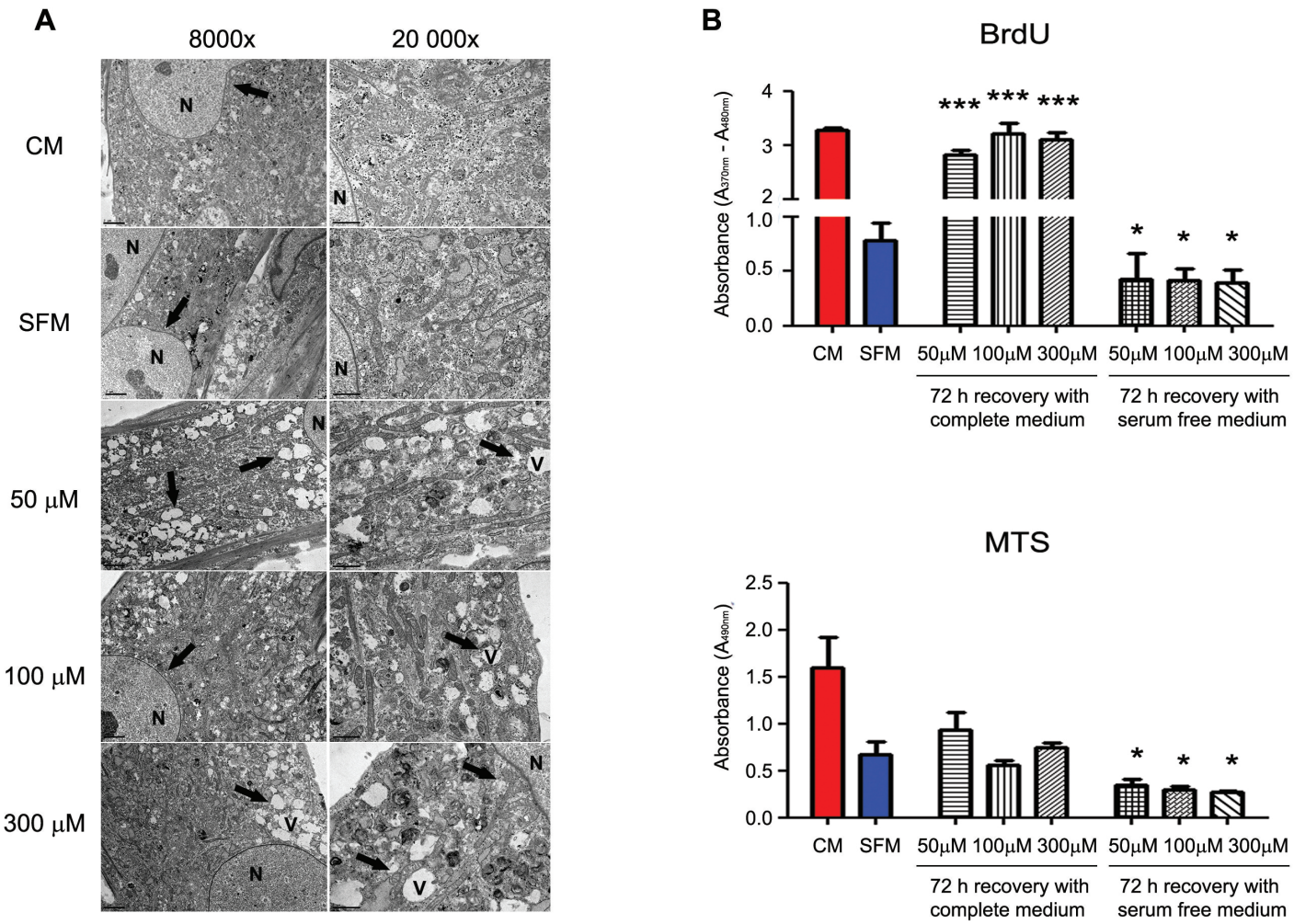
A
8000x
20 000x
CM
SFM
50 μM
100 μM
300 μM
N
V
B
BrdU
Absorbance (A370nm - A490nm)
4
3
2
1.0
0.5
0.0
***
*
CM
SFM
50μM
100μM
300μM
72 h recovery with complete medium
72 h recovery with serum free medium
MTS
Absorbance (A490nm)
2.5
2.0
1.5
1.0
0.5
0.0

C

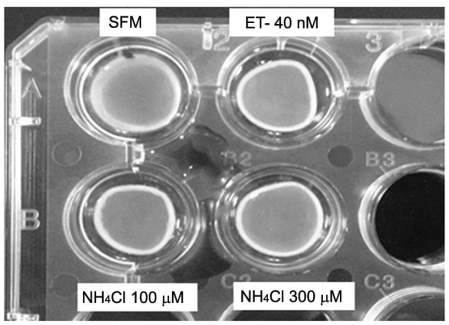
SFM
ET- 40 nM
NH4Cl 100 μM
NH4Cl 300 μM

24h

D

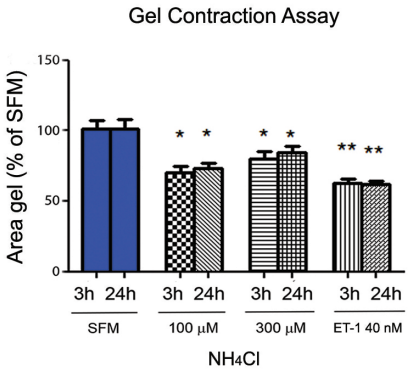
Gel Contraction Assay
Area gel (% of SFM)
150
100
50
0
3h 24h 3h 24h 3h 24h 3h 24h
SFM
100 μM
300 μM
ET-1 40 nM
NH4Cl

E

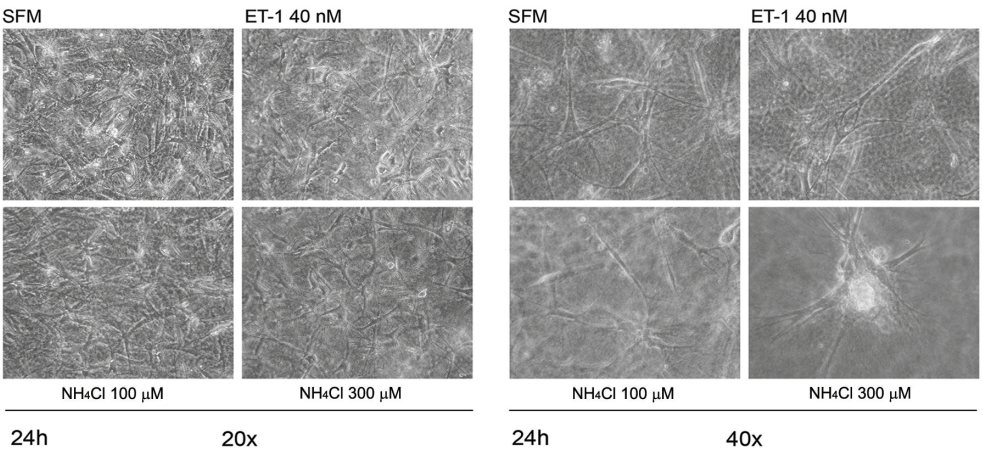
SFM
ET-1 40 nM
SFM
ET-1 40 nM
NH4Cl 100 μM
NH4Cl 300 μM
NH4Cl 100 μM
NH4Cl 300 μM
24h
20x
24h
40x

F

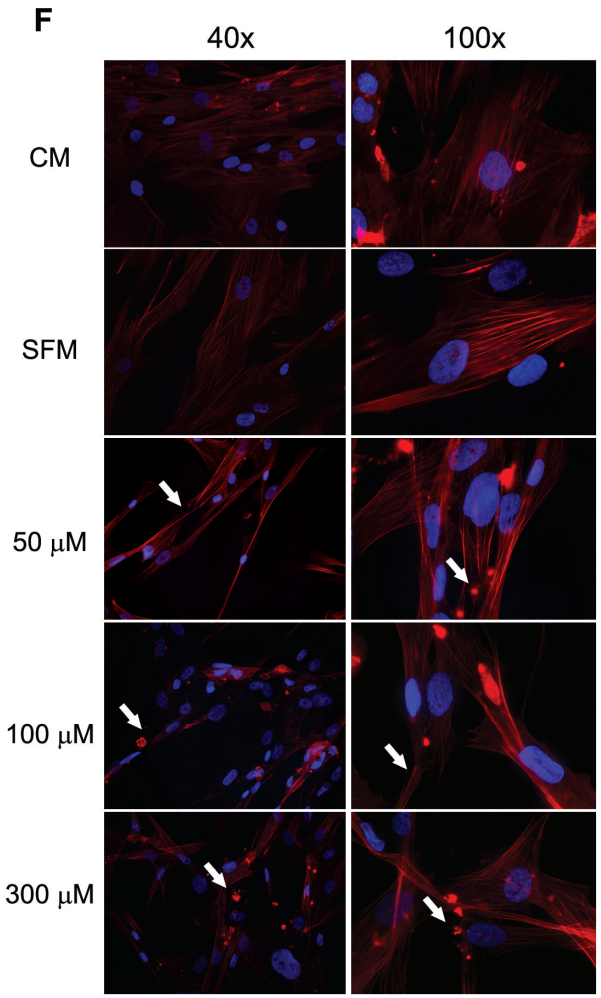
40x
100x
CM
SFM
50 μM
100 μM
300 μM

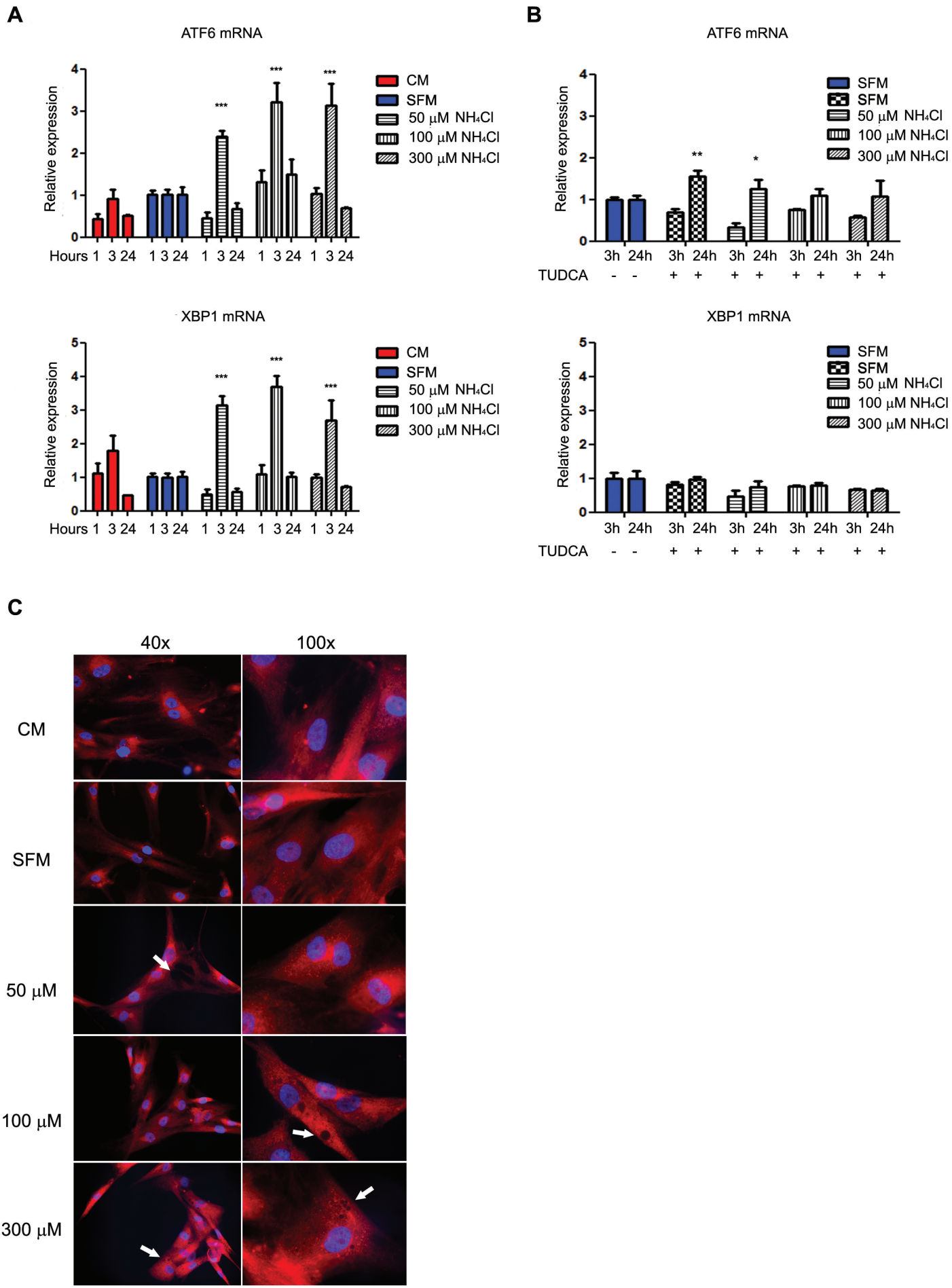
A
ATF6 mRNA
Relative expression
Hours 1 3 24 1 3 24 1 3 24 1 3 24 1 3 24
CM
SFM
50 μM NH4Cl
100 μM NH4Cl
300 μM NH4Cl
XBP1 mRNA
B
ATF6 mRNA
SFM
SFM
50 μM NH4Cl
100 μM NH4Cl
300 μM NH4Cl
3h 24h 3h 24h 3h 24h 3h 24h 3h 24h
TUDCA - - + + + + + + + +
XBP1 mRNA
C
40x
100x
CM
SFM
50 μM
100 μM
300 μM

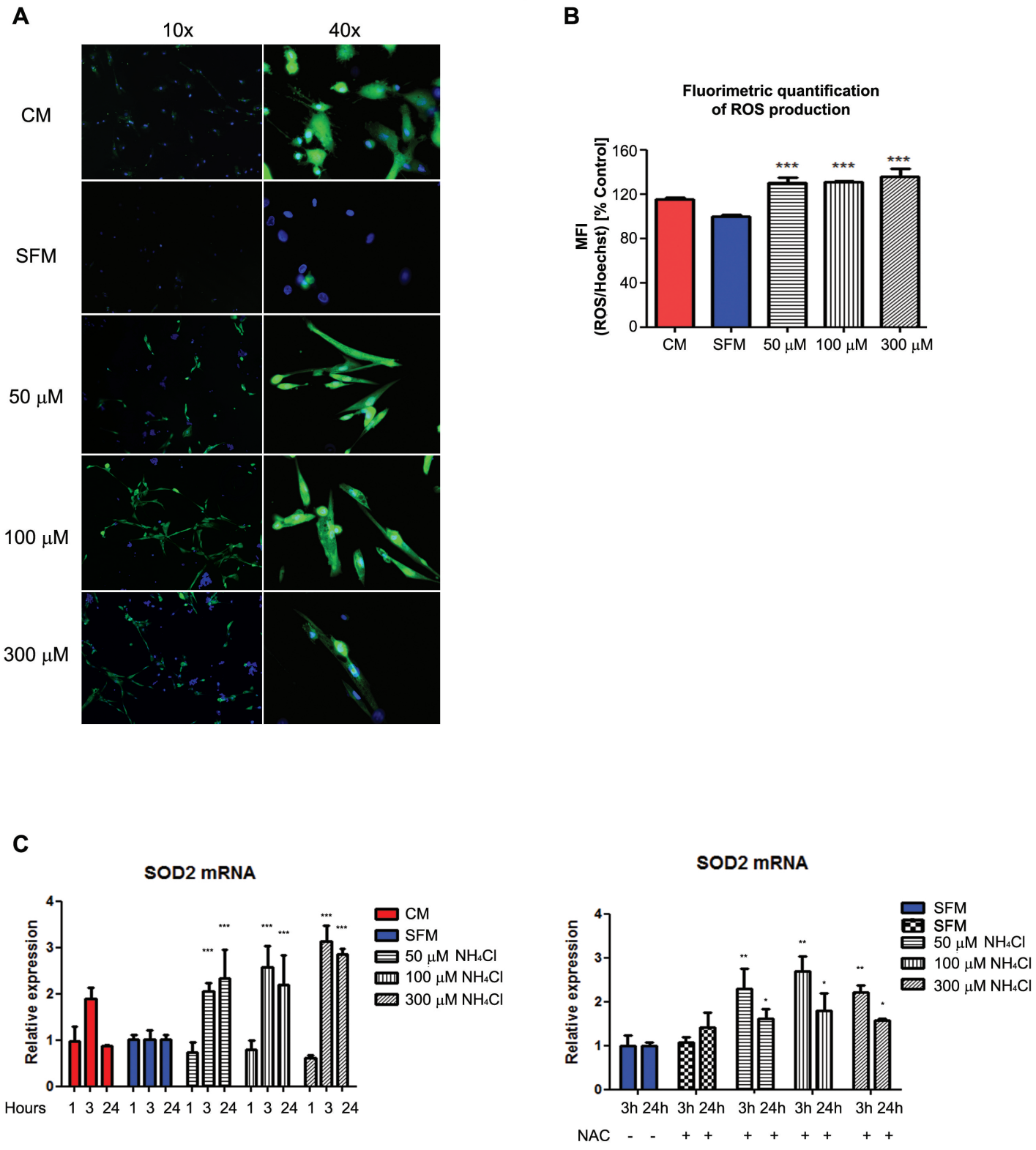
A
10x
40x
CM
SFM
50 μM
100 μM
300 μM
B
Fluorimetric quantification
of ROS production
MFI
(ROS/Hoechst) [% Control]
160
120
80
40
0
***
***
***
CM
SFM
50 μM
100 μM
300 μM
C
SOD2 mRNA
Relative expression
4
3
2
1
0
Hours
1 3 24 1 3 24 1 3 24 1 3 24 1 3 24
CM
SFM
50 μM NH4Cl
100 μM NH4Cl
300 μM NH4Cl
SOD2 mRNA
Relative expression
SFM
SFM
50 μM NH4Cl
100 μM NH4Cl
300 μM NH4Cl
3h 24h 3h 24h 3h 24h 3h 24h 3h 24h
NAC - - + + + + + + + +

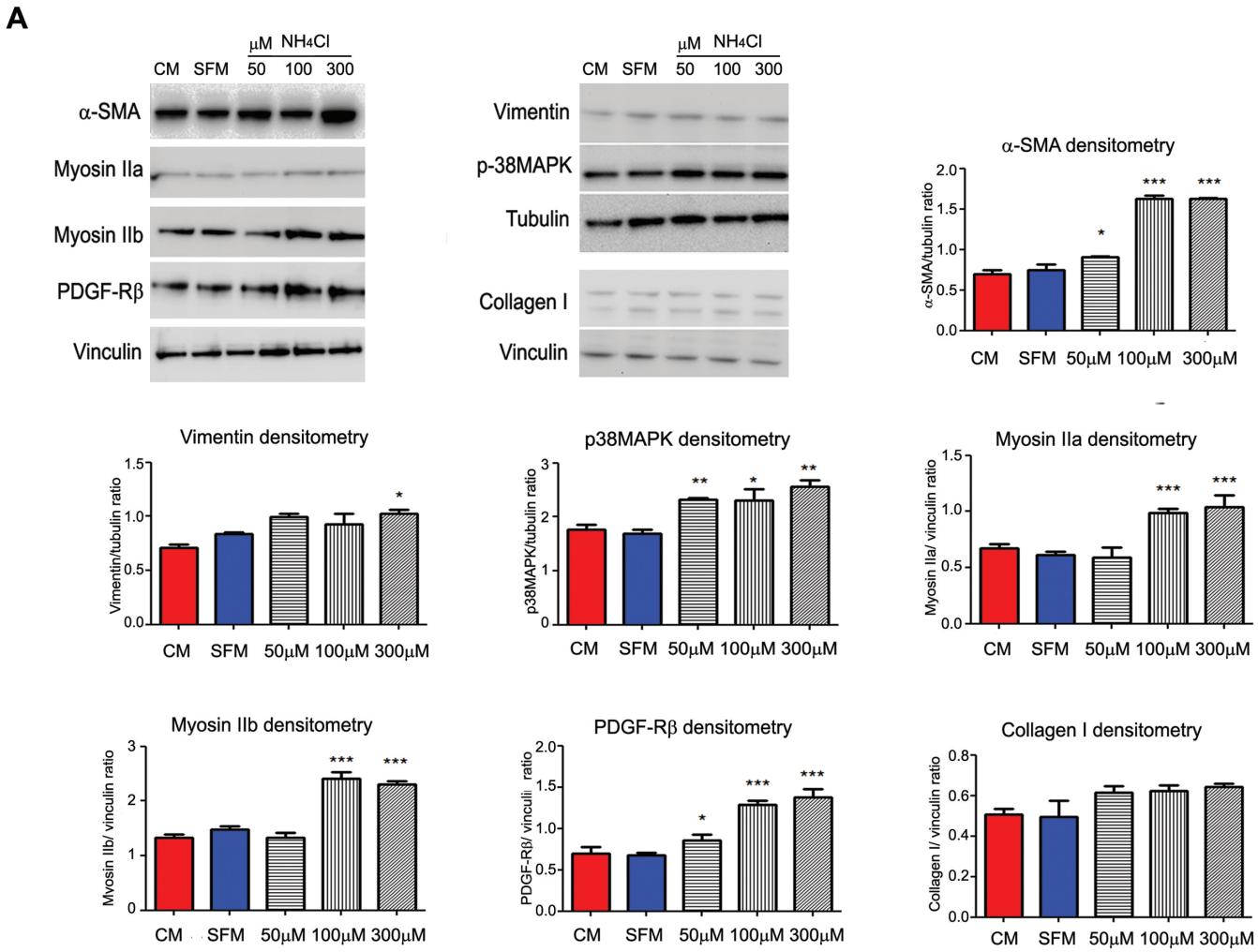
A
μM NH4Cl
CM SFM 50 100 300
α-SMA
Myosin IIa
Myosin IIb
PDGF-Rβ
Vinculin
Vimentin
p-38MAPK
Tubulin
Collagen I
Vinculin
α-SMA densitometry
α-SMA/tubulin ratio
Vimentin densitometry
Vimentin/tubulin ratio
p38MAPK densitometry
p38MAPK/tubulin ratio
Myosin IIa densitometry
Myosin IIa/ vinculin ratio
Myosin IIb densitometry
Myosin IIb/ vinculin ratio
PDGF-Rβ densitometry
PDGF-Rβ/ vinculin ratio
Collagen I densitometry
Collagen I/ vinculin ratio
CM SFM 50μM 100μM 300μM

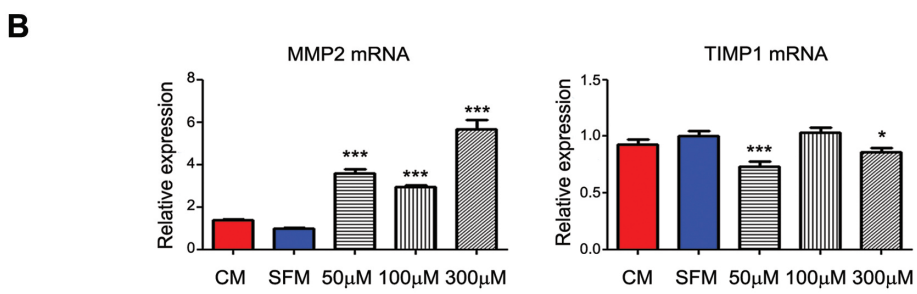
B
MMP2 mRNA
TIMP1 mRNA
Relative expression
CM SFM 50μM 100μM 300μM

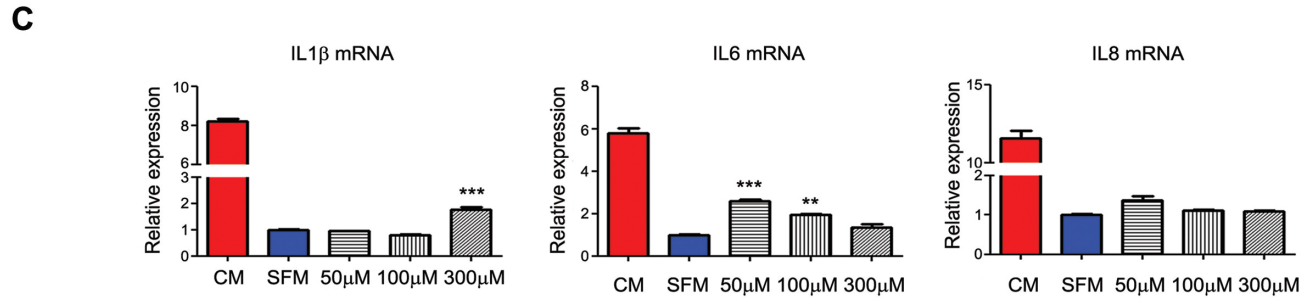
C
IL1β mRNA
IL6 mRNA
IL8 mRNA
Relative expression
CM SFM 50μM 100μM 300μM

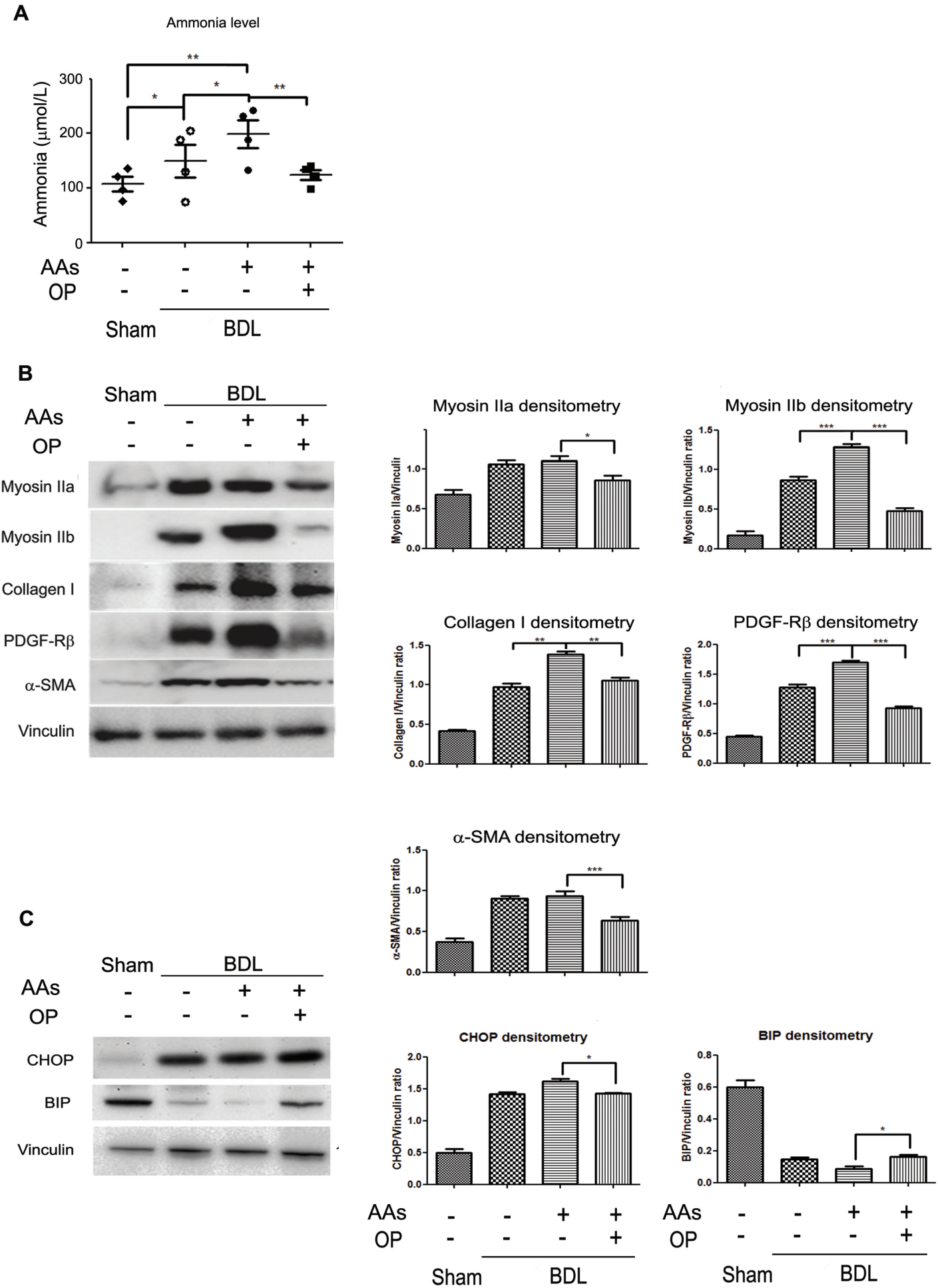
A
Ammonia level
Ammonia (μmol/L)
300
200
100
0
**
*
*
**
AAs - - + +
OP - - - +
Sham
BDL
B
Sham
BDL
AAs - - + +
OP - - - +
Myosin IIa
Myosin IIb
Collagen I
PDGF-Rβ
α-SMA
Vinculin
Myosin IIa densitometry
Myosin IIa/Vinculin
Myosin IIb densitometry
Myosin IIb/Vinculin ratio
Collagen I densitometry
Collagen I/Vinculin ratio
PDGF-Rβ densitometry
PDGF-Rβ/Vinculin ratio
α-SMA densitometry
α-SMA/Vinculin ratio
C
Sham
BDL
AAs - - + +
OP - - - +
CHOP
BIP
Vinculin
CHOP densitometry
CHOP/Vinculin ratio
BIP densitometry
BIP/Vinculin ratio
AAs - - + +
OP - - - +
Sham
BDL
AAs - - + +
OP - - - +
Sham
BDL

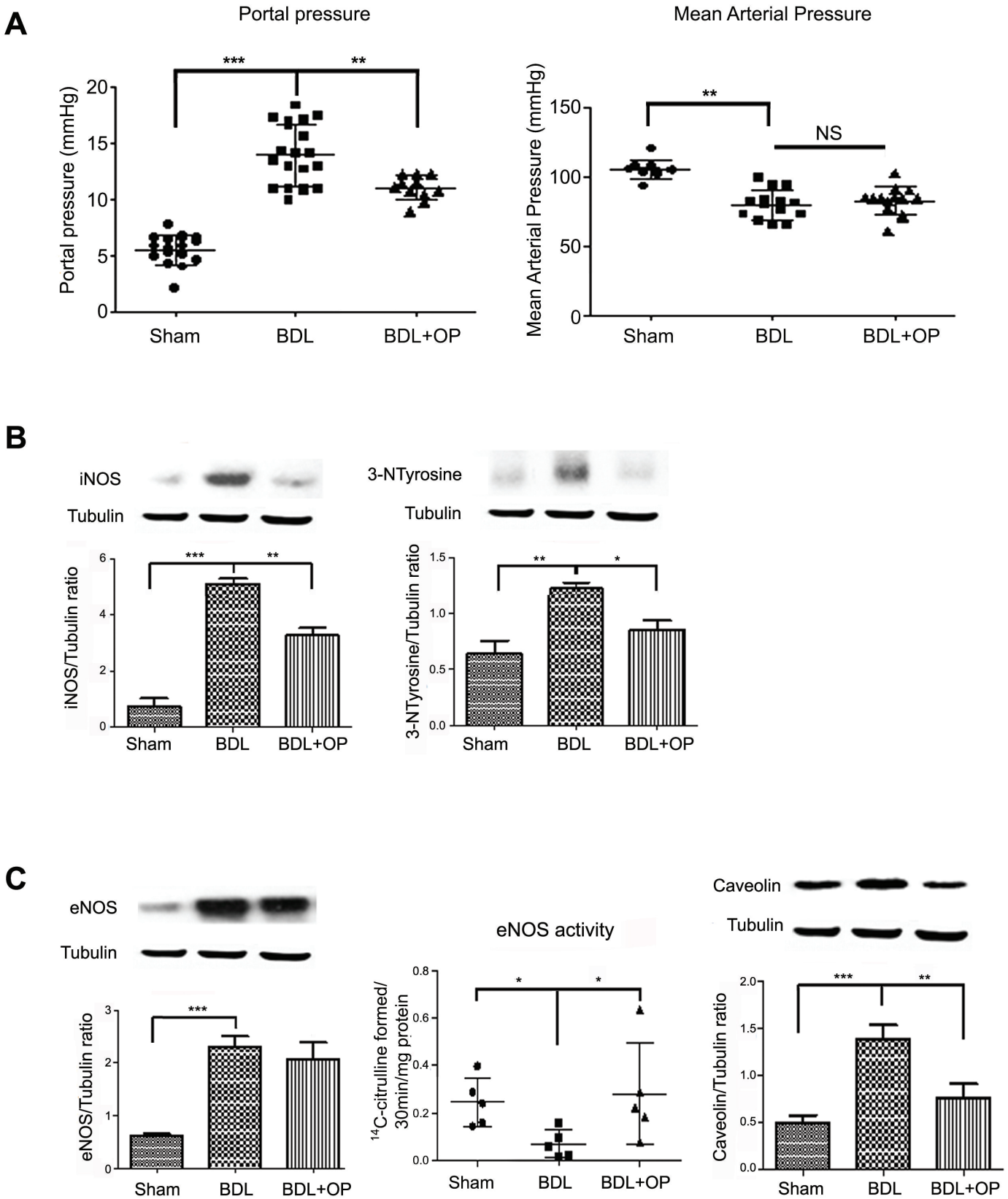
A
Portal pressure
Portal pressure (mmHg)
20
15
10
5
0
***
**
Sham
BDL
BDL+OP
Mean Arterial Pressure
Mean Arterial Pressure (mmHg)
150
100
50
0
**
NS
Sham
BDL
BDL+OP
B
iNOS
Tubulin
iNOS/Tubulin ratio
6
4
2
0
***
**
Sham
BDL
BDL+OP
3-NTyrosine
Tubulin
3-NTyrosine/Tubulin ratio
1.5
1.0
0.5
0.0
**
*
Sham
BDL
BDL+OP
C
eNOS
Tubulin
eNOS/Tubulin ratio
3
2
1
0
***
Sham
BDL
BDL+OP
eNOS activity
14C-citrulline formed/ 30min/mg protein
0.8
0.6
0.4
0.2
0.0
*
*
Sham
BDL
BDL+OP
Caveolin
Tubulin
Caveolin/Tubulin ratio
2.0
1.5
1.0
0.5
0.0
***
**
Sham
BDL
BDL+OP